Available online at www.sciencedirect.com
ScienceDirect
Comput. Methods Appl. Mech. Engrg. 284 (2015) 0–14
Computer methods in applied mechanics and engineering
www.elsevier.com/locate/cma

Two-dimensional domain decomposition based on skeleton computation for parameterization and isogeometric analysis

Jinlan Xu, Falai Chen*, Jiansong Deng

Department of Mathematics, University of Science and Technology of China, Hefei, Anhui 230026, PR China

Available online 6 October 2014

Highlights

- Two-dimensional domains are decomposed into subdomains based on skeleton computation.
- Domain partition provides better parameterization than a one-patch representation.
- The new parameterization is superior to other techniques in isogeometric analysis.

Abstract

This paper proposes a method for decomposing two-dimensional domains into subdomains for parameterization and isogeometric analysis. Given a complex domain in a plane, the skeleton of the domain is computed to guide the domain decomposition. A continuous parameterization of the domain is then obtained by parameterizing each respective subdomain. This parameterization method is applied with isogeometric analysis to solve numerical PDEs over two-dimensional domains. Examples are provided to demonstrate that the new parameterization method is superior to other state-of-the-art parameterization techniques and that it performs better in isogeometric analysis.

Keywords: Parameterization; Isogeometric analysis; Skeleton; Domain decomposition

1. Introduction

Isogeometric analysis (IGA), a method recently proposed by T.J.R. Hughes et al. [1], is a new framework for use with the finite element method (FEM) that integrates two related disciplines: computer-aided-engineering (CAE) and computer-aided-design (CAD). In IGA, geometries are precisely represented by parametric equations that remain unchanged throughout the process of refinement so that problems that are sensitive to geometric imperfections can be more readily solved [2]. IGA overcomes many problems encountered with FEM, such as mesh generation and mesh refinement. IGA has been successfully implemented in many areas, such as linear elasticity, shell problems, structural vibrations, electromagnetics, optimization and phase transition phenomena [3–6,2,7–9].

* Corresponding author. Tel.: +86 18756962203.
E-mail address: chenfl@ustc.edu.cn (F. Chen).

http://dx.doi.org/10.1016/j.cma.2014.09.026
0045-7825/

IGA uses consistent basis functions for the geometrical representation and numerical computation of PDEs. A common geometrical representation in CAD is the non-uniform rational B-splines (NURBS). However, NURBS do not have local refinement property. To facilitate adaptive solutions to PDEs, various local refinement splines have been developed, such as hierarchical splines, T-splines, PHT splines and LR splines [10–15]. Methods for constructing and analyzing suitable local refinement splines are subject to active research.

Given a computational domain over which a PDE is solved, a central problem in IGA is to compute a good parametric representation for the domain. This problem is called *parameterization*. The parameterization greatly influences the numerical accuracy and efficiency of the numerical solutions. Several approaches have been proposed to solve the parameterization problem. A common method is to use harmonic mapping to map a square to a computational domain using B-splines [16–18]. A recent study [18] proposed a method to create trivariate representations with B-splines or T-splines as an extension of the method proposed in [17]. Aigner, et al. [19] presented a variational framework for generating NURBS parameterizations of swept volumes, in which the control points can be obtained by solving an optimization problem. Another proposed method uses parameterization of a 2D domain with four planar boundary B-spline curves by solving a constraint optimization problem [20]. It has also been demonstrated that the quality of different parameterization methods can influence the solutions of the PDEs in IGA [21].

All of the above methods were proposed for finding a global parameterization of a computational domain. However, for complex domains, it is very hard or even impossible to find a single global parameterization using splines. Moreover, even when parameterization is possible, the quality of the parameterization can be very low, which is not desirable for isogeometric analysis. In this paper, we propose a totally new idea to solve this problem. First, a computational domain is decomposed into subdomains using the skeleton of the domain as a guide. Each subdomain is then parameterized to obtain a continuous parameterization for the computational domain.

This paper is organized as follows. In Section 2, we present an example to show that domain decomposition can improve the efficiency and accuracy of PDE solutions in IGA. In Section 3, a method is proposed to decompose a computational domain into subdomains. In Section 4, we present an algorithm for the parameterization of a computational domain based on the parameterization of each subdomain. Some examples of IGA based on our parameterization technique are given in Section 5. Section 6 concludes the paper with some future work.

2. Stationary heat conduction: L-shaped domain

The problem of stationary heat conduction in the L-shaped domain has been examined previously [22,23]. We will use this problem to show that domain partitioning can sometimes greatly improve the numerical accuracy of PDE solutions when using IGA.

The L-shaped domain is $\Omega = [-1, 1] \times [-1, 1] \setminus [0, 1] \times [0, 1]$ and the control equation is

$$-\Delta u = 0 \quad \text{in } \Omega,$$

with a homogeneous boundary condition for $\Gamma|_D$ and a Neumann boundary condition

$$\frac{\partial u}{\partial \mathbf{n}} = \frac{\partial f}{\partial \mathbf{n}} \quad \text{on } \Gamma_N,$$

as shown in Fig. 1, where $\mathbf{n}$ is the outer normal vector. The domain is concave, and the solution, which is singular at the origin, belongs to the space $\mathbf{H}^s = \{f \in L^2(\Omega) \mid \mathbb{D}^\alpha f \in L^2(\Omega), |\alpha| \leqslant s\}$ for $0 < s < \frac{2}{3}$. We solve the problem using IGA. We will show that different parameterizations of the L-shaped domain Ω result in different convergence properties of the solution.

The L-shaped domain Ω can be parameterized by a single biquadratic B-spline, as shown in Fig. 3. We can also partition Ω into two subdomains, as shown in Fig. 2, and parameterize each subdomain with a biquadratic B-spline to obtain a two-patch parameterization of Ω (Fig. 4). Figs. 5 and 6 show the solution and L^2 error for our parameterization. The convergence results based on these two parameterizations behave quite differently. Table 1 summarizes the convergence results based on the two parameterizations and Fig. 7 depicts the convergence plots. The numerical solution based on the parameterization after the domain decomposition converges faster than the parameterization without decomposition. The L^2 error of the solution using the former parameterization is about one tenth of the L^2 error of the latter parameterization with about the same number of degrees of freedom. This example sufficiently demonstrates that domain decomposition can improve the parameterization and numerical accuracy of

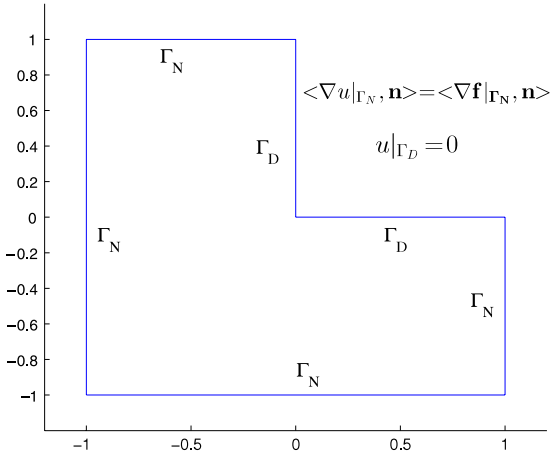

Fig. 1. L-shaped domain with boundary conditions.

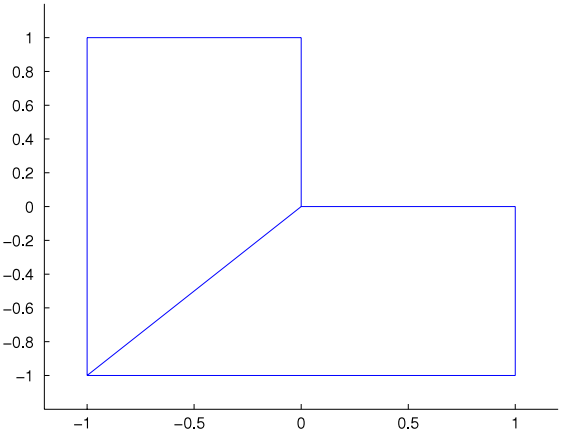

Fig. 2. L-shaped domain is partitioned into two subdomains.

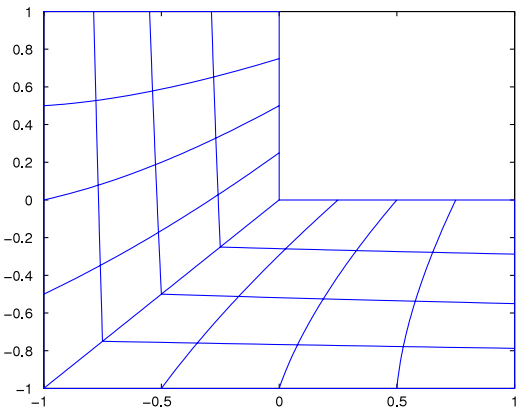

Fig. 3. Parameterization by a single biquadratic B-spline.

PDE solutions in IGA. This motivates the decomposition of complex domains into subdomains for parameterization and IGA.

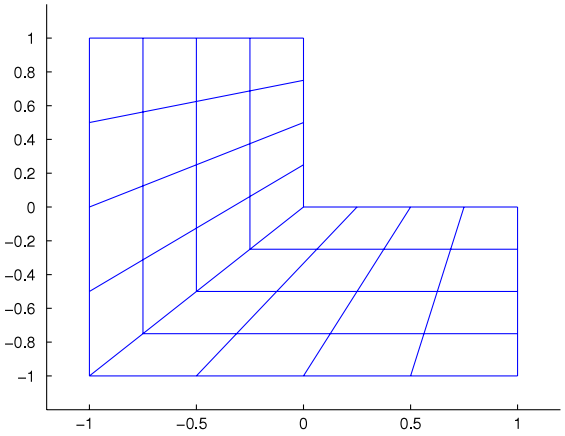

Fig. 4. Parameterization by two biquadratic B-splines.

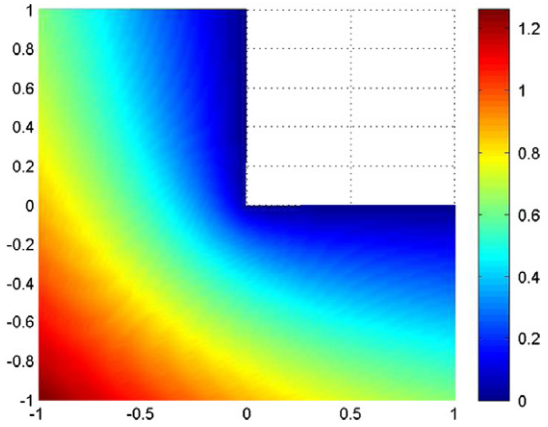

Fig. 5. The solution for two-patch parameterization.

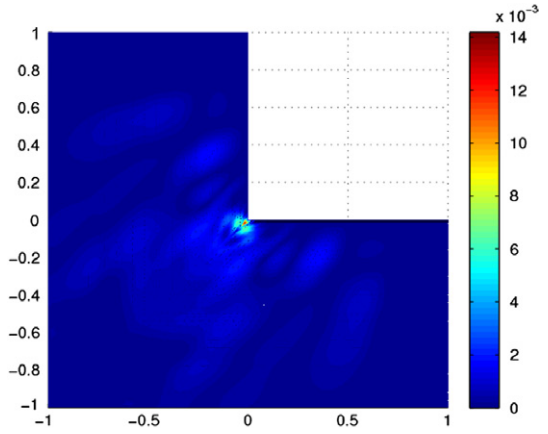

Fig. 6. The L^2 error for two-patch parameterization.

3. Decomposition of 2D domains with skeletons

Skeletons and distance information have been previously used to guide decomposition [24–28]. A hierarchical decomposition based on discrete skeletons was demonstrated previously [29]. Domakhina [30] proposed a method

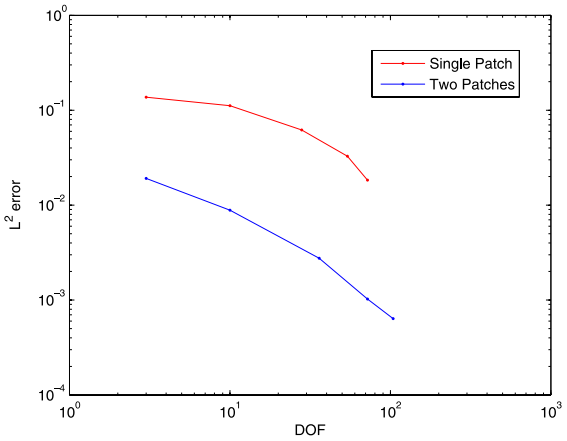

Fig. 7. Convergence plot of stationary heat conduction of the L-shaped domain.

Table 1
Convergence of the L-shaped domain heat conduction problem (n: iteration number, DOF: degree of freedom and error $= \|u_{exact} - u^h\|_{\mathbf{L}^2(\Omega)}$).

n	DOF	Error
(a) Single patch		
1	3	0.137009
2	10	0.111486
3	28	0.062023
4	54	0.0327668
5	72	0.0183534
(b) Two patches		
1	3	0.0248276
2	10	0.0125457
3	36	0.00512254
4	66	0.00210151
5	104	0.000996413

for decomposing shapes into meaningful parts reflecting shape structures based on skeleton decomposition. The decomposition represents the partition of all the edge areas of a skeleton, where the edge area of an edge l is a subset of all points closer to edge l than to the other edges. Luca [28] presented a decomposition method using the zones of influence of branch points of skeletons. However, each of the methods listed above are based on discrete representation of the whole domain. In contrast, the decomposition introduced in this paper is based on a boundary spline representation of the domain.

In the following section, the concept of skeleton is reviewed and a domain decomposition algorithm based on skeleton computation is described.

3.1. The skeleton

Skeleton (also called medial axis) is a powerful tool to represent objects. The formal mathematical definition of a skeleton is given as follows.

Definition 3.1. For a given 2D domain D, the **skeleton** of D is defined by the point set

$$S(D) = \left\{ p | D(p, B) = \|p - q_i\| = \|p - q_j\|, q_i \neq q_j, q_i, q_j \in B \right\},$$

where B is the boundary of domain D. The skeleton is the locus of the centers of circles that are tangent to the boundary curve B in two or more points, where all such circles are contained in D. The circles are called **skeleton circles**.

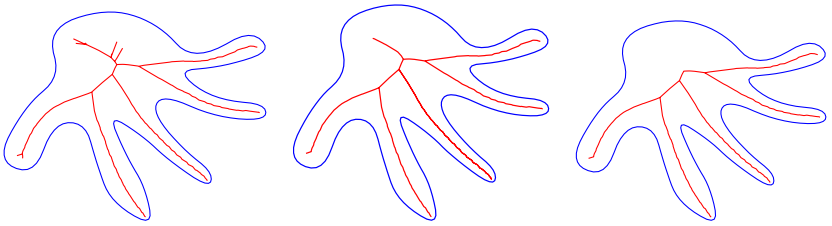

(a) Original skeleton. (b) Simplified skeleton with $\lambda = 0.01$. (c) Simplified skeleton with $\lambda = 0.05$.

Fig. 8. Skeleton of a hand shape.

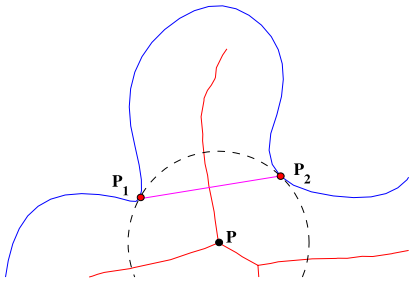

Fig. 9. For the branch point P, two contact points P_1 and P_2 of the skeleton circle at point P with the boundary curves are chosen as segmentation points.

There are many algorithms for computing skeletons of domains. A simple approach for approximating skeletons is based on the Voronoi diagram [31]. Mesh contraction was previously used to approximate the skeletons of 3D objects [32]. Additional computation methods for skeletons are described in [26]. Given a planar domain bounded by B-spline curves, we can sample the boundary curves with discrete points and apply a Voronoi diagram to compute an approximate skeleton of the domain. Schmitt [33] and Brandt [34] showed that if the sample density approaches infinity, the approximate skeleton converges to the true skeleton of the domain. An example of the skeleton computed using a Voronoi diagram is shown in Fig. 8(a).

In our application, the skeleton is only used to reflect the structure of the object, so we will remove some of the small branches that give the details of the object. The principle of simplifying skeletons involves simply cutting out the branches with lengths less than λ times the total length of the skeleton, where λ determines the number of decomposition parts ($0 < \lambda < 1$). If more parts are needed, a smaller λ can be chosen, otherwise it is acceptable for the λ to be larger. Fig. 8(b) and (c) show the simplified skeletons with different parameters λ.

3.2. Decomposition using skeletons

Because the simplified skeleton captures the structure of the domain, it can be used to guide the partitioning of the domain. Our decomposition algorithm contains two steps: decomposing the domain according to the branches of the skeleton and partitioning based on the change of the radii of the skeleton circles or the curvature change of skeleton branches. The details are described below.

3.2.1. First segmentation

Definition 3.2. A branch point is a point on the skeleton with a valence of at least three.

The valence of a point is the number of branches stretching out from the point. For example, point P in Fig. 9 is a branch point with a valence of 3. The skeleton of a domain D is connected by a series of branches. For a branch, if there is at least one end point with a valence of 1, then we associate the branch with a subdomain. A subdomain corresponding to a branch can be obtained as follows. Let P be a branch point and let C be the skeleton circle at point P. We can choose the segmentation points for the subdomain from the contact points of C with the boundary.

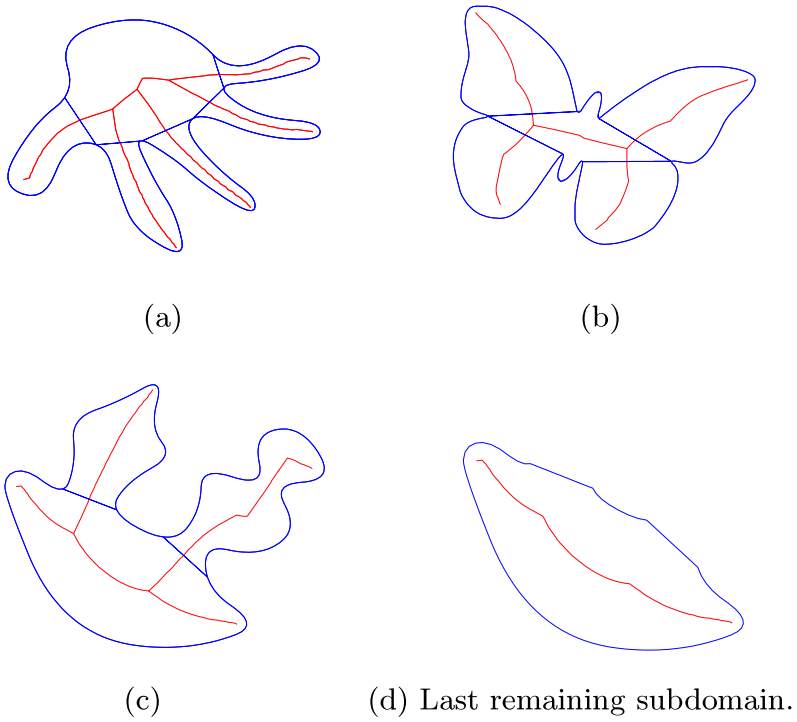

Fig. 10. First segmentation.

The segmentation points must be located on two sides of the branch. As illustrated in Fig. 9, P is a branch point and P_1 and P_2 are two contact points of C with the boundary. These points can serve as the segmentation points for the subdomain. After finding the segmentation points, a line segment connecting these two points is used as a segmentation line, and the subdomain is segmented by this line.

Domain D is decomposed as follows. Select the longest branch and segment the associated subdomain using the above method. Then, select the second longest branch and segment the subdomain associated with that branch until the remaining subdomain is almost convex or there is only one skeleton branch inside it. Here, "almost convex" means that the distance between the subdomain and its convex hull does not differ very much. With this decomposition method, the boundary of the last remaining subdomain is a curved-polygon represented with piecewise splines. Fig. 10(a)–(c) show the results of the first segmentation for three different domains, and Fig. 10(d) shows the last remaining subdomain for domain (c) after the first segmentation.

Because the boundary of the last remaining subdomain is represented by piecewise spline curves, we need to merge some of the curve segments. Without loss of generality, we may assume that all of the curve segments are of the same degree (otherwise, lower degree curves can be raised to higher degree curves through degree elevation).

Suppose two spline curves are represented as

$$C_1(u) = \sum_{i=0}^{m} P_i N_{i,1}(u) \quad \text{and} \quad C_2(u) = \sum_{i=0}^{n} Q_i N_{i,2}(u)$$

with the knot vectors

$$U_1 = [\overbrace{0, \ldots, 0}^{p+1}, u_1, u_2, \ldots, u_{m-p}, \overbrace{1, \ldots, 1}^{p+1}]$$

and

$$U_2 = [\overbrace{0, \ldots, 0}^{p+1}, \tilde{u}_1, \tilde{u}_2, \ldots, \tilde{u}_{n-p}, \overbrace{1, \ldots, 1}^{p+1}],$$

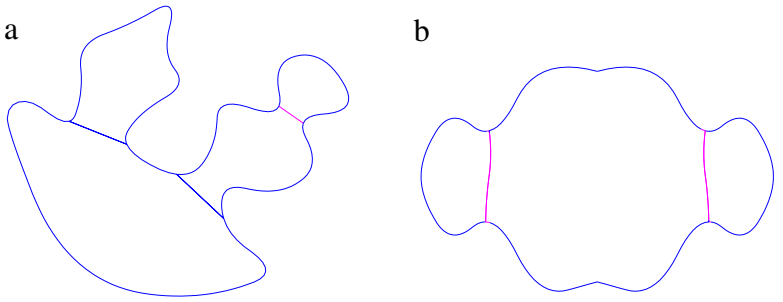

Fig. 11. Second segmentation for a large radius change.

where p is the degree of the spline curves, $P_i, i = 0, 1, \ldots, m$ and $Q_j, j = 0, 1, \ldots, n$ are control points with $P_m = Q_0$ and $N_{i,1}(u)$ and $N_{i,2}(u)$ are B-spline basis functions corresponding to the knot vectors U_1 and U_2, respectively. The new knot vector for the merged curve is

$$U = [\overbrace{0, \ldots, 0}^{p+1}, u_1, u_2, \ldots, u_{m-p}, \overbrace{1, \ldots, 1}^{p}, 1 + \tilde{u}_1, 1 + \tilde{u}_2, \ldots, 1 + \tilde{u}_{n-p}, \overbrace{2, \ldots, 2}^{p+1}]$$

which can be scaled to the interval [0, 1]. The new curve can be represented by

$$C(u) = \sum_{i=0}^{m+n} \tilde{P}_i N_i(u),$$

where $\tilde{P}_i = P_i, i = 0, \ldots, m$; $\tilde{P}_{m+j} = Q_j, j = 1, \ldots, n$, and $N_i(u), i = 0, 1, \ldots, m+n$ are B-spline basis functions corresponding to knot vector U.

3.2.2. Second segmentation

If each subdomain after the first segmentation is "almost convex", then we do not have to do anything for the second segmentation. In some situations, the subdomain obtained in the first segmentation is still not regular, e.g., the radii of the skeleton circles of a branch or the curvature of the branch vary greatly. In these cases, further segmentation can be performed if needed. The segmentation is performed at the places where large changes of radii of the skeleton circles or large branch curvatures occur. The segmentation is performed at the places where large changes of radii of the skeleton circles or large branch curvatures occur. Let $\gamma = \frac{r_{min}}{r_{max}}$, where r_{min} is the local minimum radius of the skeleton circles and r_{max} is the maximum radius of the skeleton circles respectively for a subdomain. If γ is less than some threshold, then the subdomain is further segmented at the places with local minimum skeleton circles. Similarly, let c_{max} be the local maximum curvatures of the skeleton curve, and if c_{max} is greater than some threshold, then the subdomain can be further segmented at the places with local maximum curvatures. Figs. 11–13 show the results for the second segmentations, and Fig. 14 illustrates an example of the whole process of segmentation based on skeleton.

After two steps of segmentations, we can obtain subdomains without a large distortion.

4. Parameterization

There have been many studies on parameterizing a domain with a given closed spline curve as a boundary, involving harmonic mapping and nonlinear optimization, among other strategies [20,16,35,36]. One problem that must be solved before parameterization is determining the four points on the boundary curve that correspond to the four corners of the unit square. However, in the previous studies, the authors did not provide the details on how to choose the four boundary points. Here, we provide a method to determine the four corner points.

4.1. Four corner points

For a subdomain that corresponds to one skeleton branch, there are two natural points that can be selected as corner points. These are the segmentation points that segment the subdomain from the original domain (e.g., points Q_1 and Q_2 depicted in Fig. 15). The other pair of points can be obtained by intersecting the boundary with a line perpendicular

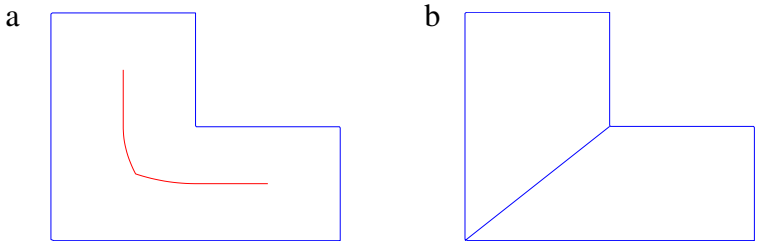

Fig. 12. Segmentation of the L-shaped domain for a large curvature change.

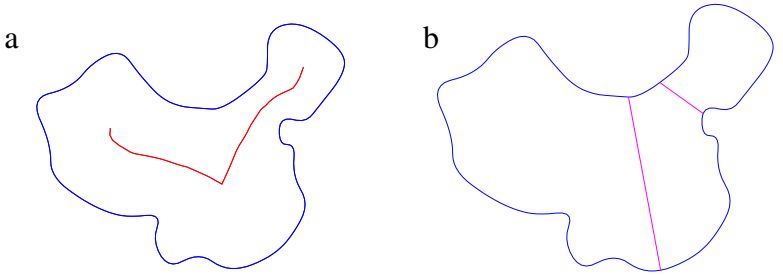

Fig. 13. The skeleton and its segmentation using the second segmentation step.

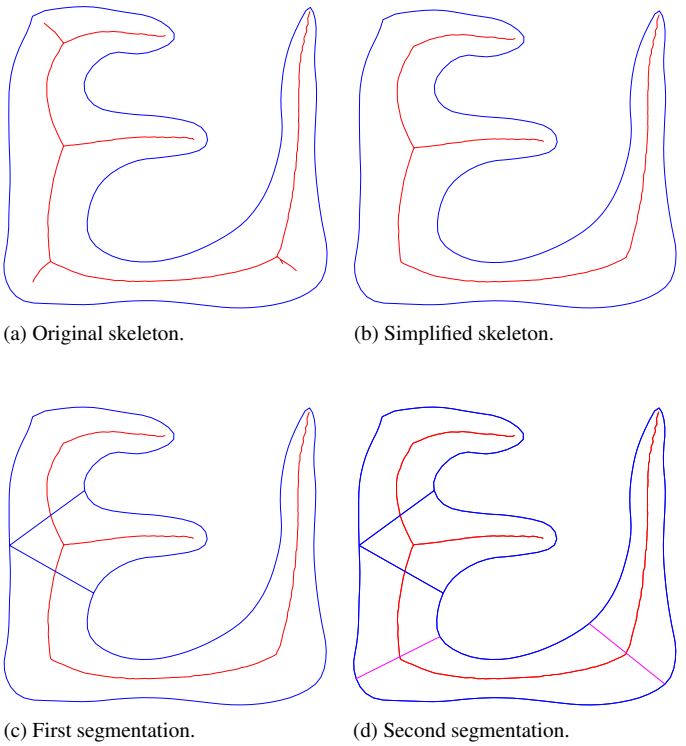

(a) Original skeleton. (b) Simplified skeleton.

(c) First segmentation. (d) Second segmentation.

Fig. 14. The whole process of segmentation based on skeleton.

to the skeleton branch (e.g., points P_1 and P_2 depicted in Fig. 15). This line can be chosen such that the opposite sides of the subdomain boundaries have similar lengths. On the other hand, one may choose singular points (i.e., the points where a curve is only C^0 continuous) on the boundary to reduce the number of singular points. For example, if there

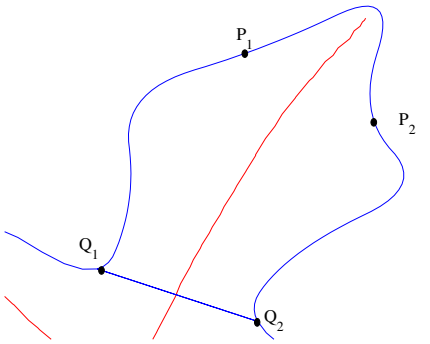

Fig. 15. Four corner points for a subdomain.

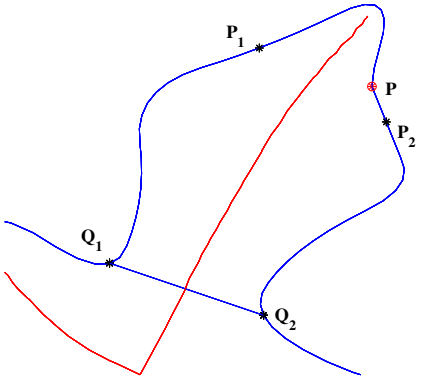

Fig. 16. The corner point P_2 is replaced by the singular point P.

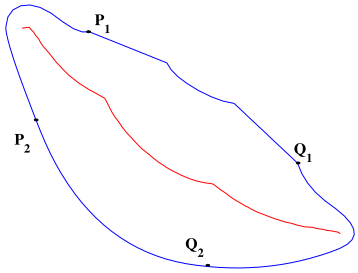

Fig. 17. Four corner points for the last subdomain in Fig. 10(d).

are singular points on the boundary, the corner points can be replaced by the nearest singular points of the boundary curve (Fig. 16).

For the last domain, the four corner points can be chosen in a similar way, followed by replacement of some of the corner points by the nearest existing corner points or singular points (Fig. 17).

4.2. The parameterization method

When the four corner points corresponding to the four corners of the unit square are fixed, four boundary curves of a B-spline representation can be determined by knot insertion. The domain can then be parameterized using any of the methods proposed in [20,16,37,38]. The criteria for choosing the optimal knot vector are described in [39–41]. In this paper, we apply the harmonic method to parameterize a subdomain. We then can obtain a continuous parameterization for the whole domain. Below, we compare our parameterization method with previous approaches, such as harmonic mapping [16,38] and nonlinear optimization [20]. While for regular domains all of the methods provide good results (see Fig. 18), for complex domains, the three methods behave quite differently. For the domain illustrated in Fig. 19,

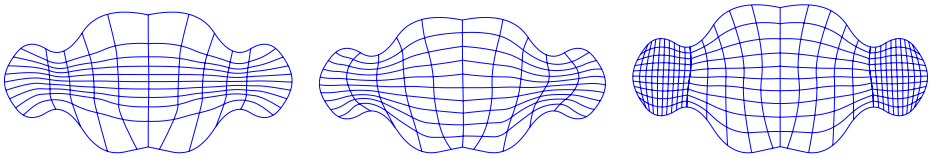

(a) Harmonic map. (b) Nonlinear optimization. (c) Our method.

Fig. 18. Comparison of different parameterization methods.

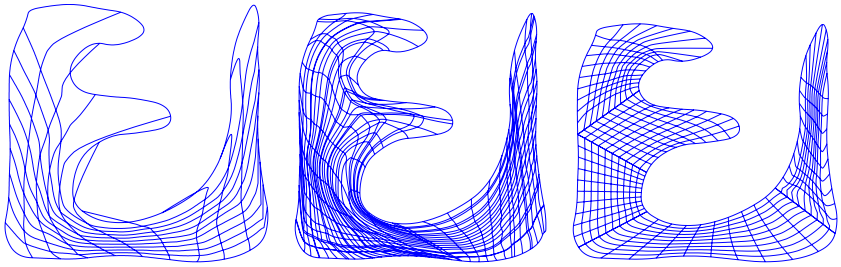

(a) Harmonic map. (b) Nonlinear optimization. (c) Our method.

Fig. 19. Comparison of different parameterization methods.

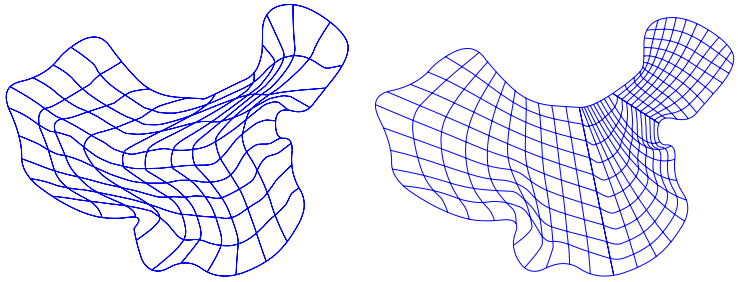

(a) Nonlinear optimization. (b) Our method.

Fig. 20. Parameterization using nonlinear optimization (a) and our decomposition-based method (b).

the harmonic map results in a parameterization with overlaps in the concave regions. The nonlinear optimization method can ensure a bijection, yet the visual quality of the parameterization is much worse than our proposed method. Fig. 20 demonstrates another example, where the map of mainland China is parameterized using different methods. In all these examples, our proposed method provides relatively good parameterization.

5. Solving PDEs with IGA

In this section, we apply the decomposition-based parameterization to solve PDEs on the domains shown in Figs. 13 and 14 (denoted as D_1 and D_2, respectively) with IGA. The numerical convergence properties are compared with the nonlinear optimization method proposed in [20].

Considering the Poisson's equation

$$\begin{cases} -\Delta w = f \\ w|_{\partial\Omega} = g \end{cases} \tag{1}$$

the weak form of Eq. (1) is given as $w(x) \in H^1(\Omega)$, $w|_{\partial\Omega} = g$, such that for all $v \in H_0^1(\Omega)$,

$$a(w, v) = f(v), \tag{2}$$

where $a(w, v) = \int_\Omega \nabla w \nabla v d\Omega$, $f(v) = \int_\Omega f v d\Omega$. Let $w = u + u_0$, where $u_0 \approx g$. Define $l(v) = f(v) - a(u_0, v)$, such that Eq. (2) is equivalent to $u \in H_0^1(\Omega)$ and $a(u, v) = l(v), \forall v \in H_0^1(\Omega)$.

In isogeometric analysis, the finite dimensional solution space $V^h \subset H_0^1(\Omega)$ is defined by the basis functions of the B-splines that represent the computational domain. Suppose the parametric equation of the computational domain Ω is

$$G(s,t) = \sum_{i=1}^{m} P_i N_i(s,t), \quad (s,t) \in [0,1]^2,$$

where P_i represents the control points and $N_i(s,t)$ are B-spline basis functions. The finite dimensional function space V_h can then be defined as

$$V^h = span\{R_i(x,y), R_i(x,y)|_\Omega = 0, i = 1,\ldots,m\}, \tag{3}$$

where $R_i(x,y) = N_i \circ G^{-1}(x,y)$.

The weak form of the isogeometric approximation becomes $u^h \in V^h$, such that for all $v^h \in V^h$,

$$a(u^h, v^h) = l(v^h), \tag{4}$$

where the approximate solution u^h takes the form $u^h = \sum_{i=1}^{n} u_i R_i(x,y)$.

In our application, the computational domain Ω consists of a set of connected components $\Omega_1, \Omega_2, \ldots, \Omega_s$ and each component is parameterized separately according to

$$G_i(s,t) = \sum_{j=1}^{m_i} P_{ij} N_{ij}(s,t), \quad i = 1,2,\ldots,s,$$

such that the solution u^h on Ω_i takes the form

$$u_i^h = \sum_{j=1}^{m_i} u_{ij} R_{ij}(x,y), \quad (x,y) \in \Omega_i,$$

where $R_{ij}(x,y) = N_{ij}(s,t) \circ G_i^{-1}(x,y)$. The term R_{ij} has support in Ω_i. To ensure that solution u^h is continuous over Ω, each common boundary $C_{ii'}$ of the two connected components Ω_i and $\Omega_{i'}$, u_i^h and $u_{i'}^h$ should be identical on $C_{ii'}$. Let $R_{ij}(x,y)$, $j = 1,2,\ldots,n_i$ be the boundary basis functions in Ω_i corresponding to the common interior boundary $C_{ii'}$. Similarly, let $R_{i'j}$, $j = 1,2,\ldots,n_i'$ be the boundary basis functions in $\Omega_{i'}$ corresponding to $C_{ii'}$. Because $C_{ii'}$ has the same parameterization for both components Ω_i and $\Omega_{i'}$, $n_i = n_{i'}$ and $R_{ij}(x,y)|_{C_{ii'}} = R_{i'j}(x,y)|_{C_{ii'}}$, $j = 1,2,\ldots,n_i$. According to the properties of B-splines, $u_i^h|_{C_{ii'}} = u_{i'}^h|_{C_{ii'}}$ if and only if

$$u_{ij} = u_{i'j}, \quad j = 1,2,\ldots,n_i.$$

From the above analysis, the solution space V^h for the whole domain can be defined as

$$V^h = \{R_{ij}, j \in I_i;\ i = 1,\ldots,s;\ R_{ij} + R_{i'j}, j \in K_{ii'},$$
$$\text{for each pair of connected components } \Omega_i \text{ and } \Omega_{i'};\}$$

Here, I_i is the index set such that each $j \in I_i$, $R_{ij}(x,y)$ is a basis function corresponding to the interior of Ω_i. $K_{ii'}$ is the index set such that for each $j \in K_{ii'}$, $R_{ij}(x,y)$ is a basis function in Ω_i corresponding to the common interior boundary $C_{ii'}$ of Ω_i and $\Omega_{i'}$, and $R_{i'j}(x,y)$ is a basis function in $\Omega_{i'}$ corresponding to the common interior boundary $C_{ii'}$.

We implemented the above scheme for two examples, where u has an exact solution $x^3 + y^3$ on domain D_1 (map of mainland China) and $x^2 + y^2$ on domain D_2, respectively. The domains are parameterized by biquadratic B-splines using the nonlinear optimization parameterization in [20] and our parameterization algorithm. The parameterization results for domain D_2 for the two methods are shown in Fig. 19(b) and (c), respectively. The parameterization results for domain D_1 are depicted in Fig. 20.

Fig. 21 shows the error plots of the solutions of the Poisson's equation (1) over the domain D_1 for the two parameterizations, where for the nonlinear optimization method (Fig. 21(a)), the error is $e_h = 0.0134045$ with $DOF = 294$ and for our decomposition based method (Fig. 21(b)), the error is $e^h = 0.00775395$ with $DOF = 260$. Fig. 22 shows the numerical errors of the solutions of the Poisson's equation over the domain D_2, where for the

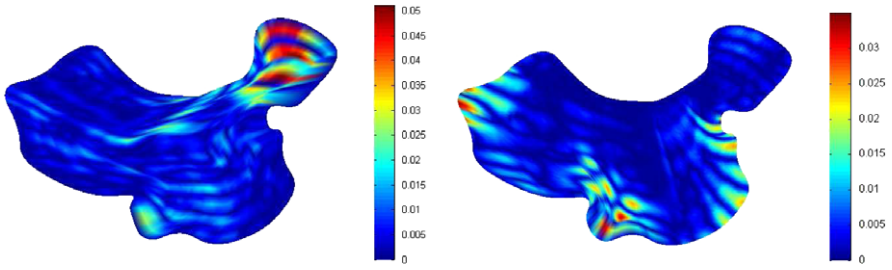

(a) Nonlinear optimization. (b) Our method.

Fig. 21. L^2 error for D_1 with two different parameterization methods.

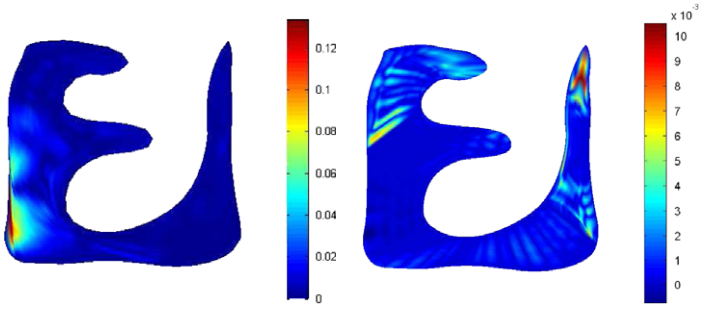

(a) Nonlinear optimization. (b) Our method.

Fig. 22. L^2 error for D_2 with two different parameterization methods.

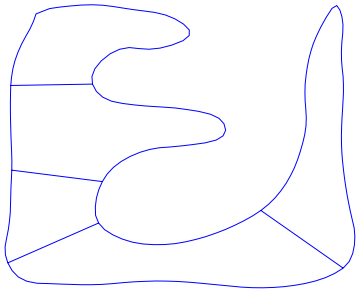

Fig. 23. Segmentation of a complex domain after optimization.

nonlinear optimization method (Fig. 22(a)), the error is $e_h = 0.0376737$ with $DOF = 702$ and for our decomposition based method (Fig. 22(b)), the error is $e^h = 0.0040979$ with $DOF = 704$. The results show that our parameterization gives better numerical accuracy with about the same number of DOFs for solving PDEs with IGA.

6. Discussion and conclusion

In this paper, we proposed a method to decompose a 2D domain into subdomains for parameterization and isogeometric analysis. In this method, the skeleton of the 2D domain is computed to guide the partition. A continuous parameterization of the domain is obtained by parameterizing each subdomain. The proposed parameterization is applied to solve numerical PDEs with isogeometric analysis. Examples are provided to demonstrate that our parameterization method is superior to other state-of-the-art parameterization techniques in terms of both the regularity of the parameterization and the numerical accuracy of the PDE solutions.

There are still problems that need to be addressed with further research. First, the parameterization method proposed in the paper may contain singular points on the boundaries similar to other parameterization methods [20]. However, it is possible to resolve this problem by decomposing a domain into more subdomains. Second, the current

method gives a topological decomposition of a 2D domain. The shape of each subdomain can be further optimized. For example, Fig. 14(d) can be modified to obtain a more regular shape, as shown in Fig. 23. Third, the current method for decomposition is not totally automatic. For example, the choice of parameter λ for cutting small branches may be different for different domains; and the choice of corner points of each subdomain may dependent on the singular points on the boundary curve. Thus, automating the decomposition is worthy of further investigation. Finally, we would like to generalize the idea in the current paper to three-dimensional geometries.

Acknowledgment

The work is supported by 973 Program 2011CB302400, the National Natural Science Foundation of China (Nos. 11031007 and 11371341) and the 111 Project (No. b07033).

References

[1] T.J.R. Hughes, J.A. Cottrell, Y. Bazilevs, Isogeometric analysis: CAD, finite elements, NURBS, exact geometry and mesh refinement, Comput. Methods Appl. Mech. Engrg. 194 (2005) 4135–4195.
[2] J.A. Cottrell, A. Reali, Y. Bazilevs, T.J.R. Hughes, Isogeometric analysis of structural vibrations, Comput. Methods Appl. Mech. Engrg. 195 (2006) 5257–5296.
[3] A. Buffa, G. Sangalli, R. Vázquez, Isogeometric analysis in electromagnetics: B-splines approximation, Comput. Methods Appl. Mech. Engrg. 199 (2010) 1143–1152.
[4] D.J. Benson, Y. Bazilevs, M.C. Hsu, T.J.R. Hughes, Isogeometric shell analysis: the Reissner–Mindlin shell, Comput. Methods Appl. Mech. Engrg. 199 (2010) 276–289.
[5] F. Auricchio, L. Beirão da Veiga, A. Buffa, C. Lovadina, A. Reali, G. Sangalli, A fully "locking-free" isogeometric approach for plane linear elasticity problems: a stream function formulation, Comput. Methods Appl. Mech. Engrg. 197 (2007) 160–172.
[6] H. Gómez, V.M. Calo, Y. Bazilevs, T.J.R. Hughes, Isogemetric analysis of the Cahn–Hilliard phase-field model, Comput. Methods Appl. Mech. Engrg. 197 (2008) 4333–4352.
[7] J. Kiendl, K.-U. Bletzinger, J. Linhard, R. Wüchner, Isogeometric shell analysis with Kirchhoff–Love elements, Comput. Methods Appl. Mech. Engrg. 198 (2009) 3902–3914.
[8] W.A. Wall, M.A. Frenzel, C. Cyron, Isogeometric structural shape optimization, Comput. Methods Appl. Mech. Engrg. 197 (2008) 2976–2988.
[9] Y.-D. Seo, H.-J. Kim, S.-K. Youn, Shape optimization and its extension to topological design based on isogeometric analysis, Int. J. Solids Struct. 47 (2010) 1618–1640.
[10] D.R. Forsey, R.H. Bartels, Hierarchical B-spline refinement, ACM SIGGRAPH Comput. Graph. 22 (1988) 205–212.
[11] J.S. Deng, F.L. Chen, X. Li, C.Q. Hu, W.H. Tong, Z.W. Yang, Y.Y. Feng, Polynomial splines over hierarchical T-meshes, Graph. Models 74 (2008) 76–86.
[12] M.A. Scott, X. Li, T.W. Sederberg, T.J.R. Hughes, Local refinement of analysis-suitable T-splines, Comput. Methods Appl. Mech. Engrg. 213 (2012) 206–222.
[13] T.W. Sederberg, J. Zheng, A. Bakenov, A. Nasri, T-splines and T-NURCCSs, ACM Trans. Graph. 22 (2003) 477–484.
[14] T.W. Sederberg, D.L. Cardon, G.T. Finnigan, N.S. North, J. Zheng, T. Lyche, T-spline simplification and local refinement, ACM Trans. Graph. 23 (2004) 276–283.
[15] T. Dokken, T. Lyche, K.F. Pettersen, Polynomial splines over locally refined box-partitions, Comput. Aided Geom. Design 30 (2013) 331–356.
[16] G. Xu, B. Mourrain, R. Duvigneau, A. Galligo, Variational harmonic method for parameterization of computational domain in 2D isogeometric analysis, in: 12th Int. Conf. on Computer-Aided Design and Computer Graphics, 2011, pp. 223–228.
[17] T. Martin, E. Cohen, R. Kirby, Volumetric parameterization and trivariate B-spline fitting using harmonic functions, Comput. Aided Geom. Design 26 (2009) 648–664.
[18] T. Martin, E. Cohen, Volumetric parameterization of complex objects by respecting multiple materials, Comput. Graph. 34 (2010) 187–197.
[19] M. Aigner, C. Heinrich, B. Juttler, E. Pilgerstorfer, B. Simeon, A.V. Vuong, Swept volume parameterization for isogeometric analysis, in: Mathematics of Surfaces XIII, in: Lecture Notes in Computer Science, vol. 5654, 2009, pp. 19–44.
[20] G. Xu, B. Mourrain, R. Duvigneau, A. Galligo, Parameterization of computational domain in isogeometric analysis: methods and comparison, Comput. Methods Appl. Mech. Engrg. 200 (2011) 2021–2031.
[21] E. Cohen, T. Martin, R.M. Kirby, T. Lyche, R.F. Riesenfeld, Analysis-aware modeling: understanding quality considerations in modeling for isogeometric analysis, Comput. Methods Appl. Mech. Engrg. 199 (2010) 334–356.
[22] M.R. Dörfel, B. Jüttler, B. Simeon, Adaptive isogeometric analysis by local h-refinement with T-splines, Comput. Methods Appl. Mech. Engrg. 199 (2010) 264–275.
[23] P. Wang, J.L. Xu, J.S. Deng, F.L. Chen, Adaptive isogeometric analysis using rational PHT-splines, Comput. Aided Design 43 (2011) 1438–1448.
[24] D. Reniers, A. Telea, Skeleton-based hierarchical shape segmentation, in: Proc. IEEE Int. Conf. on Shape Modeling and Applications, 2007, pp. 179–188.
[25] J. Lien, J. Keyser, N.M. Amato, Simultaneous shape decomposition and skeletonization, in: Proc. ACM Symposium on Solid and Physical Modeling, 2006, pp. 219–228.
[26] K. Siddiqi, S. Pizer, Medial Representations: Mathematics, Algorithms and Applications, Springer, Heidelberg, 2008.

[27] L. Serino, G.S. di Baja, C. Arcelli, Object decomposition via curvilinear skeleton partition, in: Proc. ICPR 2010, 2010, pp. 4081–4084.
[28] L. Serino, G.S. di Baja, C. Arcelli, Using the skeleton for 3D object decomposition, in: Image Analysis, in: Lecture Notes in Computer Science, vol. 6688, 2011, pp. 447–456.
[29] M. Simmons, C.H. Sequin, 2D shape decomposition and the automatic generation of hierarchical representations, Int. J. Shape Model. 4 (1998) 63–78.
[30] L.G. Domakhina, Skeleton-based segmentation and decomposition of raster pairs of shapes, Pattern Recognit. Image Anal. 20 (2010) 293–302.
[31] T.K. Dey, W.L. Zhao, Approximation medial axis as a Voronoi subcomplex, Comput. Aided Design 36 (2004) 195–202.
[32] O.K.-C. Au, C.-L. Tai, H.-K. Chu, D. Cohen-Or, T.-Y. Lee, Skeleton extraction by mesh contraction, ACM Trans. Graph. 27 (3) (2008) article no. 44.
[33] M. Schmitt, Some examples of algorithms analysis in computational geometry by means of mathematical morphological techniques, in: Proc. Workshop on Geometry and Robotics, in: Lecture Notes Comput. Science, vol. 391, Springer-Verlag, 1989, pp. 225–246.
[34] J.W. Brandt, Convergence and continuity criteria for discrete approximation of the continuous planar skeletons, CVGIP: Image Understanding 59 (1994) 116–124.
[35] M. Brovka, J.I. López, J.M. Escobar, J.M. Cascón, R. Montenegro, A new method for T-spline parameterization of complex 2D geometries, Eng. comput. 30 (2013) 457–473.
[36] P. Anděl, B. Bastl, K. Slabá, Parameterizations of generalized NURBS volumes of revolution, Eng. Mech. 19 (2012) 293–306.
[37] J. Gravesen, A. Evgrafov, D.-M. Nguyen, P. Nørtoft, Planar parameterization in isogeometric analysis, in: Lecture Notes in Computer Science, vol. 8177, 2014, pp. 189–212.
[38] T. Nguyen, B. Jüttler, Parameterization of contractible domains using sequences of harmonic maps, in: Lecture Notes in Computer Science, vol. 6920, 2012, pp. 501–514.
[39] A. Razdan, Knot placement for B-spline curve approximation, Technical Report, Arizona State University, 1999.
[40] Y. Yuan, N. Chen, S.Y. Zhou, Adaptive B-spline knots selection using multi-resolution basis set, IIE Trans. 45 (2013) 1263–1277.
[41] T. Lyche, K. Morken, Knot removal for parametric B-spline curves and surfaces, Comput. Aided Geom. Design 4 (1987) 217–230.